RSC Advances

ROYAL SOCIETY OF CHEMISTRY

www.rsc.org/advances

Graphical Abstracts

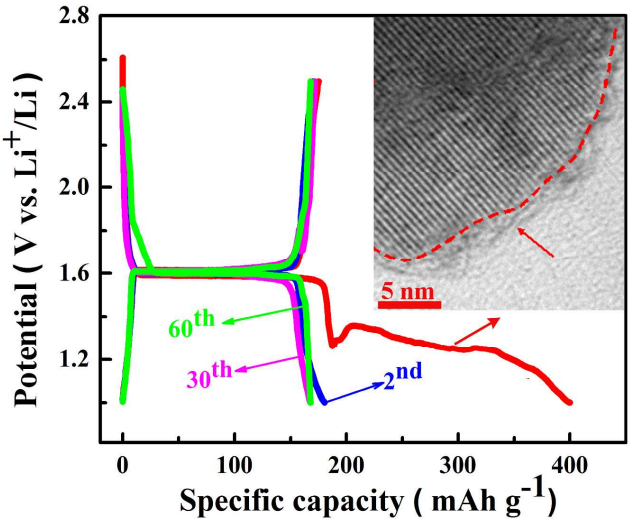

Electrochemical performance of $Li_4Ti_5O_{12}$ anode in ether electrolyte with Lithium Bis(trifluoromethanesulfonyl)Imide as lithium salt is investigated. It is firstly found that uniform solid-electrolyte interphase film can be generated on the surface of $Li_4Ti_5O_{12}$ anode in the ether electrolyte at high potential, and thus obvious enhancement of cycle stability and rate performance is obtained.

Cite this: DOI: 10.1039/c0xx00000x

www.rsc.org/xxxxxx

ARTICLE TYPE

Enhanced cycle performance of $Li_4Ti_5O_{12}$ anode in ether electrolyte induced by the solid-electrolyte interphase film

Yuxuan Zhu[a,1], Jingxia Qiu[b,c,1], Yueqing Huang[a], Po Wang[a*], Chao Lai[a*]

Received (in XXX, XXX) Xth XXXXXXXXX 20XX, Accepted Xth XXXXXXXXX 20XX

DOI: 10.1039/b000000x

The generation of uniform solid-electrolyte interphase film on the surface of $Li_4Ti_5O_{12}$ anode at the potential above 1.0 V in the ether electrolyte with Lithium Bis(trifluoromethane-sulfonyl)Imide as lithium salt are firstly reported. Significant enhancement of long cycle life can be obtained in the ether electrolyte as compared to that of conventional carbonates electrolyte. At the rate of 2 C, the discharge capacity can be stably retained at 155.4 mAh g^{-1} after 300 cycles with high capacity retention of 97.5%, which is the best result reported for the $Li_4Ti_5O_{12}$ anode with particle size above 300 nm.

Introduction

Rechargeable Li-ion batteries have been receiving extensive attention and are considered as one of the most attractive technology for application in electric vehicles and hybrid electric vehicles because of their high energy density, light weight, no memory effect and environmental benignity.[1-3] Currently, graphite is the predominant anode material for commercial lithium-ion batteries. However, the poor rate performance has hindered its application; and the existing of lithium dendrite on the electrode at the end of charge where the potential is quite close to that of lithium electrode, which may cause internal short-circuit and high safety risk in the batteries.[1-3] As an alternative to graphite, $Li_4Ti_5O_{12}$ has been investigated as an appealing material for lithium-ion battery.[3-6] It retains the advantages with low cost, low toxicity and high safety. And most importantly, lithium insertion/extraction occurs with negligible expansion of the unit cell, which makes $Li_4Ti_5O_{12}$ a promising anode.

As safety anode materials, $Li_4Ti_5O_{12}$ still encounter some serious problems, such as the poor conductivity and flatulence after long cycles.[3-16] In the past decades, extensive research mainly focus on the improvement of the rate performance of $Li_4Ti_5O_{12}$, and various nanostructure or conductivity composite $Li_4Ti_5O_{12}$ anode materials has been developed.[3,6-12] However, there are rare reports about the flatulence of $Li_4Ti_5O_{12}$-based batteries, which has been regarded as the main obstacle of the commercial application of $Li_4Ti_5O_{12}$.[13-16] For $Li_4Ti_5O_{12}$ anodes, carbonate solvent will decomposed on the surface TiO_2 which is produced from $Li_4Ti_5O_{12}$ after long cycle life, and a large amount of gas, such as CO_2 and CO, will be generated, especially at high temperature.[15,16] Such decomposition not only can generate serious flatulent phenomenon, but also can destroy the stable cycle performance of $Li_4Ti_5O_{12}$. It has been suggested that the surface coating will be effective method to prohibit the contact between the carbonate and surface of active materials, and then restrict the generation of gas in the batteries.[13-16] However, it is technology difficult to produce a uniform and adequate coating layer, and always a complex synthesis process is needed, limiting their practical applications. Thus, the key to address the flatulent problem is how to building a uniform and adequate surface coating layer via simple strategy.

Solid-electrolyte interphase (SEI) has been suggested as the crucial key to the stability and durability of Li-ion batteries.[16-19]During the charging process, the SEI layer can be generated due to the reductive decomposition of the electrolyte at the surface of electrode. The SEI film is a Li^+ conductor but insulator of electron transport, and thus can prevents further electrolyte decomposition to improve the cycle life performance of the Li-ion batteries.[16-19] For $Li_4Ti_5O_{12}$ anodes, the SEI film is also an ideal coating layer to separate the electrode from the electrolyte, and thus effectively restrict the flatulence of $Li_4Ti_5O_{12}$-based batteries. Although it will be a big challenge since the formation of SEI film happens in a low potential, the strategy of producing a SEI layer on the surface of $Li_4Ti_5O_{12}$ is still appealing. In Lithium-sulfur batteries, the ether electrolyte (1,3-dioxolane and Dimethoxyethane) with Lithium Bis(trifluoromethane-sulfonyl)Imide (LiTFSI) is used as lithium salt. The 1,3-dioxolane in the electrolyte is easy to open loop in the presence of acids, such as H^+ and Lewis acid (metal ions). Thus, the ring-opening reaction of 1,3-dioxolane is possible after the generation of Ti^{3+} during the discharge process for the $Li_4Ti_5O_{12}$ anodes, and then can produce a surface layer. Follow on such design, in this work, we first investigate the electrochemical performance of $Li_4Ti_5O_{12}$ in the ether electrolyte with LiTFSI as lithium salt. Surprisingly, a uniform surface coating layer is generated during the initial cycle, and obviously enhanced cycle performance is obtained.

Experimental

2.1. Materials characterization

The commercial $Li_4Ti_5O_{12}$ were characterized by an X-ray diffractometer (XRD, Model LabX-6000, Shimadzu) with CuKα radiation. The morphology and structure of the $Li_4Ti_5O_{12}$ were examined by a scanning electron microscopy (SEM, JOEL, JSM-

7001F), and a high-resolution transmission electron microscopy (HR-TEM) (FEI Model Tecnai 20) with an acceleration voltage of 200 kV.

2.2 Electrochemical measurements

The anode slurry were prepared by mixing 70 wt.% $Li_4Ti_5O_{12}$, 20 wt.% acetylene black and 10 wt.% binder (Polytetrafluorothelyene, PTFE) in ethanol. Then the slurry was grinded and punched into round disks and dried at 60 ºC for 12 h in vacuum oven. The average mass of the electrodes was ca. 4 mg cm^{-2}.

The half cells were assembled with the $Li_4Ti_5O_{12}$ electrode as the working electrode, lithium metal sheet as reference electrode and counter electrode, copper was used as current collector and porous polypropylene film acted as separator. Two different kinds of electrolytes were used in the system. One is a mixture solution composed of 1.0 M $LiPF_6$ in 1:1 (w/w) ethylene carbonate (EC)/ dimethyl carborbonate (DMC), designated as $LiPF_6$/carbonates. Another is 1.0 M LiTFSI dissolved in Dimethoxyethane (DME) and dioxolane (DOL) (1:1, volume), designated as LiTFSI/ethers. The charge/discharge process of $Li_4Ti_5O_{12}$ electrode in different electrolyte system were performed at different C rates in the voltage range of 1.0–2.5 V vs. Li/Li^+ using Land-CT2001A battery tester (Wuhan, PRC). Electrochemical impedance spectra (EIS) were collected using Solartron 1287 electrochemical workstation. A perturbation of 5 mV was applied and data collected under PC control (custom software) from 100 kHz to 10 mHz.

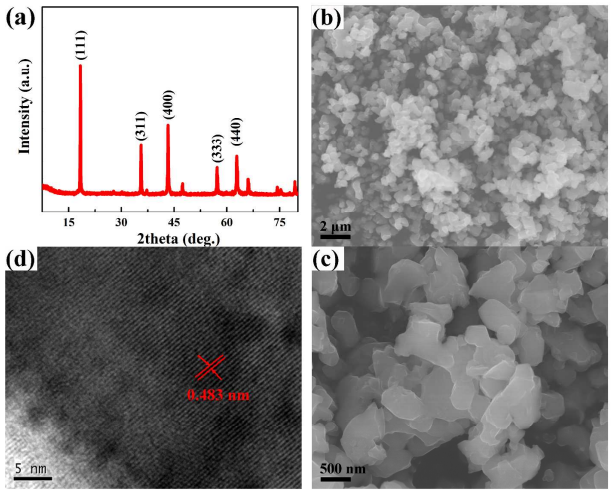

Fig.1 XRD pattern (a), SEM (b,c) and TEM (d) images of commercial $Li_4Ti_5O_{12}$.

Results and discussion

The morphology and structure of commercialized $Li_4Ti_5O_{12}$ is characterized by the XRD pattern, SEM and TEM images, as displayed in Fig.1. From Fig.1a, the powder XRD pattern agrees well with JCPDS (card No. 49-0207) of $Li_4Ti_5O_{12}$, revealing that the sample has a single-phase cubic structure in Fd3m space group.[4-13] As shown in the low- and high- magnification SEM images in Fig. 1b and 1c, it is clearly shown the $Li_4Ti_5O_{12}$ has uniform size distribution with a diameter in the range of 300–500 nm. The HRTEM images indicate the entire particle of $Li_4Ti_5O_{12}$ is highly crystallized with a lattice spacing of 0.483 nm, which is consistent with the (111) planes of the $Li_4Ti_5O_{12}$ in Fig. 1d.

Lithium-ion battery cells were assembled to test the electrochemical performances of the $Li_4Ti_5O_{12}$ in LiTFSI/ethers and $LiPF_6$/carbonates electrolyte systems. The typical voltage profile of the electrodes at 1st cycle, 2nd cycle, 30th and 60th cycle in $LiPF_6$/carbonates and LiTFSI/ethers electrolytes were presented at a current density of 0.1 C (1 C = 175 mA g^{-1}) in Fig. 2a and 2b. In conventional carbonates electrolyte, a distinct discharge and charge potential plateaus around 1.51 and 1.57 V can be observed, which suggesting good kinetic process. This is a typical feature of two-phase lithium insertion and extraction processes corresponding to the transformation of $Li_4Ti_5O_{12}$ and $Li_7Ti_5O_{12}$.[4-13,20,21] Nevertheless, in the ether electrolyte, similar discharge-charge curves can be observed except that an additional long flat plateau appeared at the potential around 1.2 V in the initial discharging process, similar to the reductive decomposition of electrolyte on the surface of graphite anode below 1 V.[22,23] For the titanium-based anode materials, especially in the nanoscale, the continuous decomposing of electrolyte and forming of unstable SEI film is a common phenomenon, leading to the serious gassing issues.[24,25] Thus, the long distinguishing discharge plateau may correspond to the formation process of stable SEI film on the $Li_4Ti_5O_{12}$.

In addition, it was observed that the sample in LiTFSI/ethers electrolyte performed much better than that of $LiPF_6$/carbonates. The initial discharge capacity in the ether electrolyte was 431.9 mAh g^{-1}, and a high capacity of 169.5 mAh g^{-1} was preserved after 60th cycles at 0.1 C. However, in carbonates electrolyte system, the sample demonstrated an initial discharge capacity of 184 mAh g^{-1}, and which gradually decrease to 158.0 mAh g^{-1} at the 60th cycles.

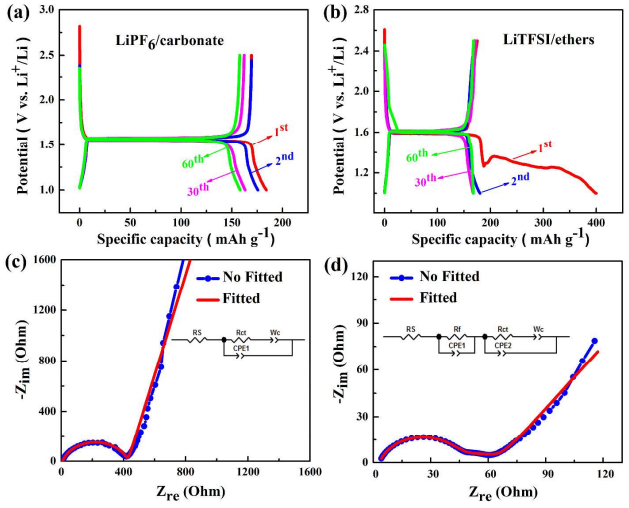

Fig.2 The discharge-charge curves and $Li_4Ti_5O_{12}$ in different electrolytes (a,b); Nyquist plots of $Li_4Ti_5O_{12}$ anodes in $LiPF_6$/carbonates (c) and LiTFSI/ethers (d) electrolyte systems after initial discharge-charge process at the rate of 0.1 C.

To illustrate the discharge mechanisms of $Li_4Ti_5O_{12}$ in the ether electrolyte, EIS tests were measured at open-circuit potential and at discharged state to 2.5 V, and the results are given in Fig. 2c and 2d. For the $Li_4Ti_5O_{12}$ anode in the carbonate electrolyte, it can be seen that the Nyquist plot consists of one

depressed semicircle at high frequencies and a straight line at low frequencies before discharge. The diameter of high frequencies semicircle refers to the charge transfer resistance, relating to the electrochemical reaction at the electrode-electrolyte, while the straight line is attributed to Warburg element, relating to the Li-ion diffusion in the $Li_4Ti_5O_{12}$. [18,22,26-28] For the $Li_4Ti_5O_{12}$ in the ether electrolyte, An additional semicircles can be observed, and it suggests the formation of solid electrolyte interphase (SEI) on the surface of $Li_4Ti_5O_{12}$ electrode, which may result from the decomposition or polymerization of ether solvent illustrated below.[27,28] The fitting the results of EIS are given in Table S1, and it is found that the charge transfer resistance of the cell using ether electrolyte is much smaller than that of carbonate electrolyte (R_{ct}), and this is mainly due to the high conductivity of LiTFSi/ether electrolyte (R_s), thus leading to a better electrochemical performance.[29] The change of Li-ion diffusion coefficient D_{Li} in different electrolytes also can be calculated from the low frequency liner warburg regions according to the following equation:[30,31]

$$D_{Li}=1/2[(V_m/FA\delta_w)*d_E/d_x]^2$$

where V_m is the molar volume of $Li_4Ti_5O_{12}$, F is the Faraday constant and A is the total contact area between the electrolyte and the electrode. δ_w is the Warburg coefficient which was obtained from the warburg region of impedance response as shown in Fig. S1, while the d_E/d_x is obtained from the slopes of the initial charge curves. The calculated Li-ion diffusion coefficient in ether electrolyte is about 35.8 times higher that in the carbonate electrolyte.

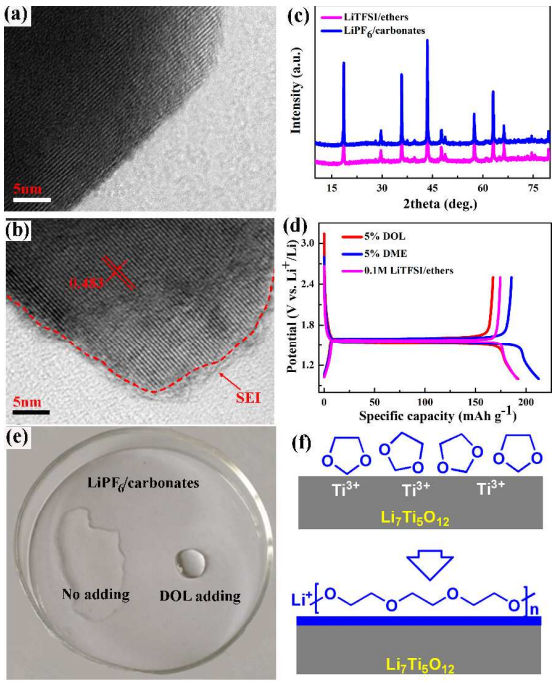

Fig.3 TEM images of $Li_4Ti_5O_{12}$ anodes in LiPF6/carbonates (a) and LiTFSI/ethers (b) electrolyte systems after initial cycle at the rate of 0.1C; XRD patterns (c) of the $Li_4Ti_5O_{12}$ electrode after 300 cycles at the rate of 2C; Initial discharge-charge curves (d) of $Li_4Ti_5O_{12}$ anodes in LiPF6/carbonates with different additives; the comparison (e) of LiPF6/carbonates electrolyte with and without DOL adding; the possible mechanisms of the formation of SEI film (f).

The evidence of the formation of SEI film on the surface of $Li_4Ti_5O_{12}$ can be straightforwardly observed by the HRTEM images in Fig. 3a and 3b. As shown, after first cycle, a homogeneous thin layer of stable SEI was produced outside the crystal lattice in the electrode in ether electrolyte, while there is no surface layer that can be observed for the electrode in the carbonate electrolyte. The *d*-spacing of the $Li_4Ti_5O_{12}$ after the formation of SEI film is ca. 0.48 nm, suggesting that there is no phase change in the ether electrolyte. The structural stability of $Li_4Ti_5O_{12}$ in ether electrolyte can be further confirmed by the XRD patterns after various cycles. Fig. 3c presents XRD patterns of both the charged electrodes in LiTFSI/ethers and $LiPF_6$/carbonates electrolytes directly after acetone wash after 300 cycles at the rate of 2 C. All diffraction peaks of materials can be indexed to a single-phase cubic spinel structure in Fd3m space group, suggesting that the crystal structure of $Li_4Ti_5O_{12}$ has not been changed after long cycles.[4-13] By considering all the results above, it can be concluded that uniform SEI film can be generated on the surface of $Li_4Ti_5O_{12}$ in the ether electrolyte, and such a coating layer is favorable to producing high cycle stability.

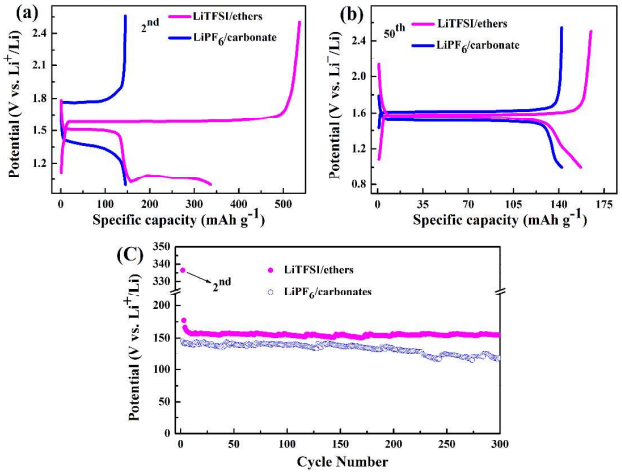

Fig.4 The second (a) and 50th (b) discharge-charge curves of $Li_4Ti_5O_{12}$ anode in different electrolytes; cycle curves (c) of $Li_4Ti_5O_{12}$ anode in different electrolytes.

A comprehensive comparison of the electrochemical behaviors of $Li_4Ti_5O_{12}$ in various electrolytes is given in Fig. 3d to explain how the formation of SEI on the surface of electrode facilitates the performance of elelctrode. As presented, with DOL and DME and LITFSI salt adding in the $LiPF_6$/carbonates electrolytes, respectively, the $Li_4Ti_5O_{12}$ electrodes show similar discharge-charge curves with that in the $LiPF_6$/carbonates electrolytes, and there is no additional potential plateau as that in the pure LiTFSI/ethers electrolytes, suggesting that the formation of SEI film may relate to the amount of solvents in the electrolyte. To further illustrate the formation mechanisms of SEI film, the DOL and $LiPF_6$/carbonates electrolytes are mixed with a volume ratio of 1:1. As shown in Fig. 3e, the mixture becomes extremely viscous after 6h resulting from the polymerization of DOL, [32,33] while there are no change happened by adding DME. Accordingly, one possible reaction mechanisms are proposed in Fig. 3f. As demonstrated, after discharged to 1.5 V, Ti^{3+} will generate, act as initiator for the polymerization of DOL, and at last produce uniform coating layer on the surface of the $Li_4Ti_5O_{12}$ electrode.[32-34] Such a hypothesis mainly base on the instability of

DOL during the discharge process,[34] especially in the presence of Ti^{3+}. More experiments are still needed to clearly clarify the formation mechanisms of SEI in the ether electrolyte.

As discussed above, $Li_4Ti_5O_{12}$ in ether electrolyte shows a much lower interface resistance, and the formation of SEI film is favorable to obtain stable cycle performance.[18,35] Accordingly, the rate performance (2C) of the $Li_4Ti_5O_{12}$ in ether electrolyte is also investigated. Fig. 4a is the 2nd discharge-charge curves of the $Li_4Ti_5O_{12}$ electrode in ether and carbonate electrolyte. As shown, there is an obvious plateau at around 1.05 V using the ether electrolyte, suggesting the formation of SEI film. Different from its discharge-charge curves at the rate of 0.1 C, there is a noticeable overcharge phenomenon. This may be because that it hardly forms a fully covering and stable SEI film on the surface of electrode during fast discharge-charge process, and there are still exposed catalytic active regions. During the charge process, the decomposition of electrolyte and dissociation of SEI film may happen together, leading to the overcharge phenomenon. Such a hypothesis can be confirmed by the EIS results after different cycles at the rate of 2C. As presented in Fig. S2, after the initial two cycles, the straight line turns to be an arc-like profile in the low-frequency region that represents a finite Nernst diffusion process in a thin layer,[36] suggesting the gradual formation of surface film on the electrode. After initial several cycles, the overcharge will disappear as shown in Fig. 4b. Furthermore, the cell using the ether electrolyte demonstrate a much lower polarization potential as compared to that using conventional carbonates electrolyte, indicating better kinetic process. The cycling performance profiles of $Li_4Ti_5O_{12}$ in LiTFSI/ethers and $LiPF_6$/carbonates electrolyte at constant current density of 2 C are given in Fig. 4c. As presented, in the initial 100 cycles, both electrolytes can support a superior cycle performance. However, after that, the discharge capacity will decrease rapidly in the carbonate electrolyte, while there is basically no capacity decay in the ether electrolytes. The stable reversible capacity of electrode in LiTFSI/ethers is 159.5 mAh g^{-1} (6^{th}), and can be retained at 155.4 mAh g^{-1} after 300 cycles with the retention of 97.5 %. While it present only 118 mAh g^{-1} for $LiPF_6$/carbonates after 300 cycles. Therefore, the electrode in LiTFSI/ethers electrolyte exhibits significantly enhanced cycle performance due to the formation of SEI film.[17-19]

Conclusions

In summary, we demonstrated a novel and simple strategy, using ether electrolyte with Lithium Bis(trifluoromethane-sulfonyl)Imide as lithium salt, to produce a uniform SEI layer on the surface of $Li_4Ti_5O_{12}$ electrode at high potential. The formation of SEI film can be confirmed by the discharge-charge curves, EIS and HRTEM images. The electrodes using ether electrolyte exhibits a much better cycle and rate performance than conventional carbonates electrolyte. The excellent cycle stability can be ascribed to the formation of uniform SEI layer which can successfully separate the electrode from electrolyte to maintain the structure stability of electrode, and furthermore maybe can prohibit the flatulent phenomenon in the $Li_4Ti_5O_{12}$-based batteries. At the rate of 0.1C, the capacity can be stability retained at 169.5 mAh g^{-1} in ether electrolyte, while it is only 158.0 in carbonates electrolyte. When the rate increasing to 2 C, a high discharge capacity of 155.4 mAh g^{-1} still can be obtained after 300 cycles in the ether electrolyte, and the capacity retention can reach to 91.7% as compared to that at the rate of 0.1 C. However, in conventional carbonates electrolyte, the cell shows a poor cycle life, and the capacity is ca. 118 mAh g^{-1} after 300 cycles.

Acknowledgements

This work has been supported by the Chinese National Science Funds (No. 51202094); the Priority Academic Program Development of Jiangsu Higher Education Institutions.

Notes and references

[a] School of Chemistry and Chemical Engineering, and Jiangsu Key Laboratory of Green Synthetic Chemistry for Functional Materials, Jiangsu Normal University, Xuzhou, Jiangsu 221116, P. R. China, Email: laichao@jsnu.edu.cn;
[b] Institute for Energy Research, Jiangsu University, Zhenjiang, Jiangsu, 21203, P. R. China;
[c] School of Chemistry and Molecular Biosciences, Faculty of Science, the University of Queensland, Brisbane, QLD 4072
[1] Both authors contributed equally to this work.

1 W. Xu, J.L. Wang, F. Ding, X.L. Chen, E. Nasybutin, Y.H. Zhang and J.G. Zhang, *Energ. Environ.* Sci., 2014, **7**, 513.
2 J. Jiang, Y.Y. Li, J.P. Liu, X.T. Huang, C.Z. Yuan and X.W. Lou, *Adv. Mater.* 2012, **24**, 5166.
3 G.N. Zhu, Y.G. Wang and Y.Y. Xia, *Energ. Environ. Sci*., 2012, **5**, 6652.
4 Y.Q. Wang, L. Gu, Y.G. Guo, H. Li, X.Q. He, S. Tsukimoto, Y. Ikuhara and L.J. Wan, *J. Am. Chem. Soc*., 2012, **134**, 7874.
5 L. Yu, H.B. Wu and X.W. Lou, *Adv. Mater.,* 2013, ***25,*** 2296.
6 X. Hao and B.M. Bartlett, *Adv. Energy Mater.*, 2013, **3**, 753.
7 X.L. Jia, Y.F. Kan, G.Q. Ning, Y.F. Lu and F. Wei, *Nano Energy*, 2014, **10**, 344.
8 Y. Oh, S. Nam, S. Wi, J. Kang, T. Hwang, S. Lee, H.H. Park, J. Cabana, C. Kim and B. Park, *J. Mater. Chem. A*, 2014, **2**, 2023.
9 J. Liu, K Song, P.A. Aken, J. Maier and Y. Yu, *Nan*o Lett., 2014, **14**, 2597.
10 H.H. Xu, X.L. Hu, Y.M. Sun, W. Luo, C.J. Chen, Y.H. Huang, *Nano Energy*, 2014, **10**, 163.
11 C.F. Lin, X.Y. Fan, Y.L. Xin, F.Q. Cheng, M.O. Lai, H.H. Zhou and L. Lu, *J. Mater. Chem. A,* 2014, **2**, 9982.
12 C. Lai, Y.Y. Dou, X. Li and X.P. Gao, *J. Power Sources,* 2010, **195**, 3676.
13 W. Li, X. Li, M.Z. Chen, Z.W. Xie, J.X. Zhang, S.Q. Dong and M.Z. Qu, *Electrochim. Acta,* 2014, **139**, 104.
14 L. Wei, Z.Y. Wu, H.Z. Luo, R.S. Song and F. Li, *J. Electrochem. Soc.,* 2015, **162**, A3038.
15 R. Bernhard, S. Meini and H.A. Gasteiger, *J. Electrochem. Soc.*, 2014, **161**, A497.
16 Y.B. He, B. Li, M. Liu, C. Zhang, W. Lv, C. Yang, J. Li, H.D. Du, B. Zhang, Q.H. Yang, J.K. Kang and F. Kang, *Sci. Rep.*, 2012, **2**, 913.
17 S. Bhattacharya, A.R. Ahmet and A.T. Alpas, *Carbon*, 2014, **77**, 99.
18 Y.B. He, M. Liu, Z.D. Huang, B. Zhang, Y. Yu, B.H. Li, F.Y. Kang and J.K. Kim, *J. Power Sources*, 2013, **239**, 269.
19 M.D. Bhatt and C. O'Dwyer, *J. Electrochem. Soc.*, 2014, **161**, A1415.

20 K.S. Park, A. Benayad, D.J. Kang, and S.G. Doo, *J. Am. Chem. Soc*., 2008, **130**, 14930.

21 M. Kitta, T. Akita, S. Tanaka, M. Kohyama, *J. Power Sources*, 2014, **257**, 120.

22 C. Liao, K.S. Han, L. Baggetto, D.A. Hillesheim, R. Custelcean, E.S. Lee, B.K. Guo, Z.H. Bi, D.E. Jiang, G.M. Veith, E.W. Hagaman, G.M. Brown, C, Bridges, A. Manthiram, S. Dai and X.G. Sun, *Adv. Energy Mater.*, 2014, **4**, 1301368.

23 P. Murmann, P. Niehoff, R. Schmitz, S. Nowak, H. Gores, Nikaolailgnatiev, P. Sartori, M. Winter and R. Schmitz, *Electrochim. Acta*, 2013, **114**, 658.

24 C.P Han, Y.B He, H.F Li, B.H Li, H.D. Du, X.Y. Qin and F.Y. Kang, *Electrochim. Acta*, 2015, **157**, 266.

25 S. Brutti, V. Gentili, H. Menard, B. Scrosati and P. G. Bruce, *Adv. Energy Mater*., 2012, **2**, 322.

26 C. Lai, X.L. Cao, X.C. Yuan, Y.L. Wang and S.H. Ye, *Solid State Ionics*, 2013, **249-250**, 151.

27 C.L. Wei, W. He, X.D. Zhang, S.J. Liu, C. Jin, S.K. Liu, Z. Huang, *RSC Adv.,* 2015, **5**, 28662.

28 M. Umeda, K. Dokko, Y. Fujita, M. Mohamedi, I Uchida and J.R. Selman, *Electrochim. Acta,* 2001, **47**, 885.

29 K. Xu, *Chem. Rev.,* 2004, **104**, 4303.

30 Y.G. Wang, H.M. Liu, K.X. Wang, H. Eiji, Y.R. Wang and H.S. Zhou, *J. Mater. Chem.,* 2009, **19**, 6789.

31 Ji-Y. Shin, J.H. Joo, D. Samuelis and J. Maier, *Chem. Mater.,* 2012, **24**, 543.

32 N. Nemoto, Y. Ito and T. Endo, *J. Polym. Sci. Pol. Chem.*, 2003, **41**, 699.

33 NE. Djelali, D. Aliouche, L.D. Oubeka and G. Pierre, *Asian J. Chem.*, 2006, **18**, 1839.

34 L. Kong, H. Zhan, Y.J. Li and Y.H. Zhou, *Electrochem. Commun.*, 2007, **9**, 2557.

35 J.J. Xu, Y.Y. Hu, T. Liu and X.D. Wu, *Nano Energy*, 2014, **5**, 67.

36 Y. Liu, X. Huang, Q.Q. Qiao, Y.L. Wang, S.H. Ye, X.P. Gao, *Electrochim. Acta,* 2014, **147**, 696.